Theor Appl Climatol
DOI 10.1007/s00704-011-0562-1

ORIGINAL PAPER

Hydrometeorological application of an extratropical cyclone classification scheme in the southern United States

J. C. Senkbeil · D. M. Brommer · I. J. Comstock · T. Loyd

Received: 4 August 2011 / Accepted: 18 November 2011

Abstract Extratropical cyclones (ETCs) in the southern United States are often overlooked when compared with tropical cyclones in the region and ETCs in the northern United States. Although southern ETCs are significant weather events, there is currently not an operational scheme used for identifying and discussing these nameless storms. In this research, we classified 84 ETCs (1970–2009). We manually identified five distinct formation regions and seven unique ETC types using statistical classification. Statistical classification employed the use of principal components analysis and two methods of cluster analysis. Both manual and statistical storm types generally showed positive (negative) relationships with El Niño (La Niña). Manual storm types displayed precipitation swaths consistent with discrete storm tracks which further legitimizes the existence of multiple modes of southern ETCs. Statistical storm types also displayed unique precipitation intensity swaths, but these swaths were less indicative of track location. It is hoped that by classifying southern ETCs into types, that forecasters, hydrologists, and broadcast meteorologists might be able to better anticipate projected amounts of precipitation at their locations.

1 Introduction

Several regional and synoptic scale extratropical cyclone (ETC) climatologies have been constructed in the United States with various emphases on manual methods (Bowie and Weightman 1914; Pettersen 1956; Klein 1957; Reitan 1974; Colucci 1976; Zishka and Smith 1980; Whittaker and Horn 1981, 1984.) The collective results of these studies contributed to the identification of distinct regions of ETC cyclogenesis and cyclolysis regions with preferred cyclone tracks. These results proliferated through introductory physical geography and meteorology textbooks throughout the United States, commonly highlighting four to eight ETC tracks: the Alberta Clipper (Thomas and Martin 2010), Colorado Low (Bierly and Winkler 2001), Texas Low, and Gulf Low (Lewis and Hsu 1992). The Texas Low and Gulf Low track through the southern United States while other types of ETCs track north of the region. Through years of personal observation in the southern United States, the existence of multiple modes of southern ETCs in addition to or within the traditional Texas and Gulf Lows began to be questioned by the authors.

From approximately December through March, ETCs in the southern United States are a regular occurrence, varying considerably in both intensity and frequency. They are generally not as intense or destructive as tropical cyclones that impact the region between June and November; however, they are more frequent than tropical cyclones in most years. While true in the northeastern United States (Kunkel et al. 1999), a series of strong southern ETCs in the cold season could have the same economic impact as one or two tropical cyclones of minimal hurricane intensity. The impacts of southern ETCs may also rival the damage attributed to ETCs in the northeast United States (Noreasters). Even though southern ETCs are generally less intense than Noreasters, southern ETCs are frequently preceded or accompanied by a range of weather hazards, such as severe thunderstorms, tornados, flooding, coastal erosion, freezing rain, sleet, and, occasionally, even blizzards. All of these hazards were associated with the 1993 March Superstorm (Kocin et al. 1995). Furthermore, winter storms appear to be increasing in intensity since 1980 in the southern United States (Changnon 2007).

J. C. Senkbeil (✉) · D. M. Brommer · I. J. Comstock · T. Loyd
Department of Geography, University of Alabama,
Box 870322, Tuscaloosa, AL 35487, USA
e-mail: jcsenkbeil@bama.ua.edu

Published online: 10 December 2011

Precipitation from ETCs also plays an important role in assessing hydroclimatic variability and calculation of the regional water budget (Mennis 2001; Peters et al. 2003). Hayden (1988) devised flood climate zones classifying much of the southern United States into a pattern dominated by seasonal baroclinicity and warm season barotropic flood regimes. Under Hayden's classification, the region is capable of flooding from a variety of mechanisms throughout the year. Hirschboeck (1991) discussed regional peak flooding seasonality. The peak for the majority of the southern United States is winter/spring, associated with ETC formation and passage. Gamble (1997) further elaborated on these findings and divided the southeastern United States into five peak flood seasonality regions.

Recently, automated or statistical ETC climatologies have been conducted in Europe (Campins et al. 2000, 2010; Maheras et al. 2001; Bartholy et al. 2006; Kouroutzoglou et al. 2010), the North Pacific (Mesquita et al. 2010), and the southern hemisphere (Simmonds and Keay 2000; Buckley and Leslie 2004; Bernardes Pezza and Ambrizzi 2005). Furthermore, there has been a global emphasis on methodological issues with datasets and tracking methods (Wernli and Schwierz 2006; Froude et al. 2007; Raible et al. 2008), including the United States. A few studies have emphasized Noreasters (Davis et al. 1993; Hirsch et al. 2001; Kocin and Uccellini 2004) and the classification of ETCs in the north-central and eastern United States (Zielinski 2002). Eichler and Higgins (2006) created an ETC climatology for North America with a particular focus on El Niño Southern Oscillation (ENSO) precipitation impacts while Frankoski and DeGaetano (2011) recently completed a precipitation climatology for winter storms on the east coast USA. In the southern United States, there have been two notable ETC studies (Businger et al. 1990 and Curtis 2006). Businger et al. (1990) analyzed precipitation totals of 66 winter low pressure systems during the 1960–1983 time period over the Gulf of Mexico and identified three primary storm tracks. Curtis (2006) studied the spatial variability in cyclogenesis locations for southern ETCs during El Niño, neutral, and La Niña winters. El Niño winters are characterized by more numerous and intense storms in the southeastern United States and also a greater variety of cyclogenesis locations.

This research has two objectives: (1) identify common characteristics of ETCs in the southern United States and develop schemes for analyzing and discussing these storms and their precipitation impacts; and (2) apply the classification schemes for hydrometeorological purposes. With southern ETCs playing such a vital role in the climate and water balance of the region, these classification schemes may assist forecasters and hydrologists to more accurately predict and anticipate precipitation totals associated with types of ETCs.

The majority of this article is devoted to explaining the ETC classification schemes and resulting storm types from the first objective. Thus, the article contains several subsections within the "Methods" section, which includes criteria for storm selection, a summary of manual and automated classification procedures, and a description of geographic information system (GIS) procedures for calculating and analyzing precipitation totals. The "Results and discussion" section is split into discussions of both manual and statistical classification schemes, a brief assessment of storm frequency and ENSO phase, and an analysis of precipitation distribution and intensity associated with each storm type.

2 Methods

2.1 Storm selection

Eighty-four southern ETCs that attained a central pressure <1,008 hPa were identified during the period 1970–2009. This pressure value was chosen to eliminate numerous storms >1,008 hPa primarily due to the very brief life spans and weaker structures of these storms. Storm selection involved a few basic criteria and the use of two datasets for cross-referencing to eliminate any potential error. The process of storm selection started with visual analysis of daily weather maps from National Oceanic and Atmospheric Administration's (NOAA) daily weather map project (http://docs.lib.noaa.gov/rescue/dwm/data_rescue_daily_weather_maps.html) and then transitioned to more specific analyses using National Centers for Environmental Prediction/National Center for Atmospheric Research (NCEP/NCAR) Reanalysis Data (Kalnay et al. 1996).

Step 1 in storm selection was defining a strong southern ETC. Strong ETCs were defined as having central pressures <1,008 hPa with at least 75% of their circulation within the study region (25–35°N and 105–75°W) (Fig. 1). A value of 75% of circulation was determined by importing the pressure values into a GIS and measuring the total circumference of the storm <1,008 hPa and the circumference <1,008 hPa contained within the grid. A percentage was then taken between these two values to qualify at 75%. The ETC season was defined as 1 December to 31 March, when strong ETCs were common within the region. ETCs also occur in November and April, however, very few of the storms in these months were 75% within the grid with most passing to the north.

Identifying southern ETCs was accomplished by manual analysis of daily NOAA weather maps to ensure that all possible storms were identified. In this first step, all potential storms were recorded, including storms that skimmed the northern or eastern boundaries of the study area with minimal impacts. A total of 114 storms were identified in this step.

Next, each storm was analyzed using the NCEP/NCAR reanalysis dataset at 6-h increments (Kalnay et al. 1996).

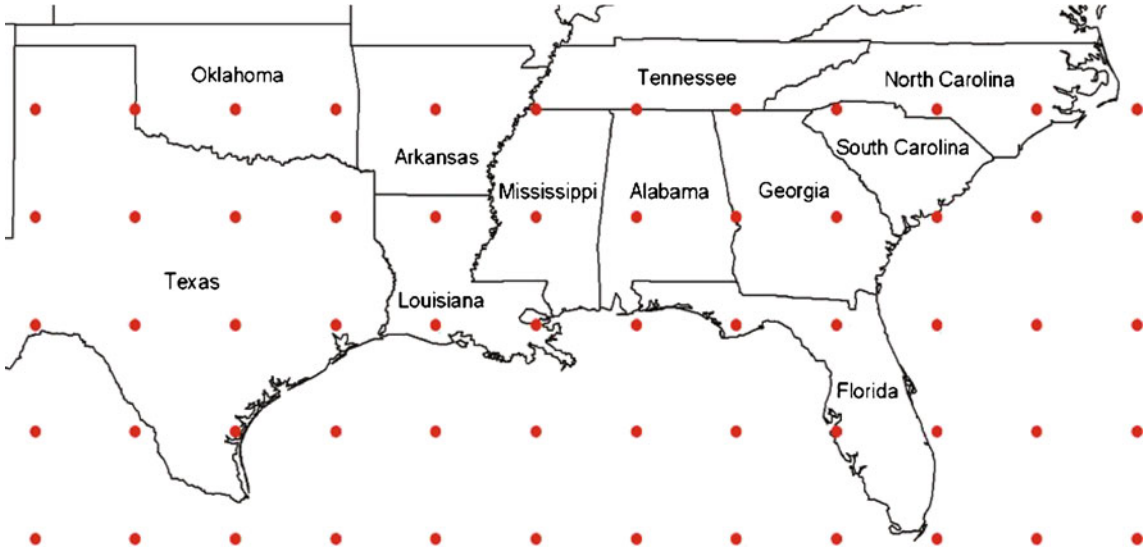

Fig. 1 Study region with 2.5°×2.5° latitude and longitude grid from NCEP/NCAR re-analysis data

These data were downloaded and analyzed using a GIS within the study region at 1 hPa increments from 980 to 1,008 hPa (http://esrl.noaa.gov/psd/data/composites/hour/). This visualization technique trimmed the dataset to 84 storms that were concentric low pressure areas <1,008 hPa and at least 75% contained within the study region. Although the authors recognize a certain degree of subjectivity in the manual techniques used, we also feel that it is potentially more thorough than automated extraction procedures that were also considered.

2.2 Manual classification

Manual classification was performed by binning storm origin locations and storm destination locations on a latitude/longitude grid connected via common tracks. In our manual classification, we identified five distinct formation regions for southern ETCs. Storms were binned according to these regional associations. The five manual regions are: (1) Rio Grande, (2) Gulf, (3) Plains, (4) Southeast, and (5) Florida. Common tracks varied within each region with many disparate and also overlapping patterns (Fig. 2).

2.3 Statistical classification

Statistical classification involved principal components analysis (PCA) followed by two types of cluster analysis. These methods have been used effectively in previous studies (Esteban et al. 2006; Hart et al. 2006; Fragoso and Gomes 2008; Sheridan et al. 2008; Neal and Phillips 2009). Before describing the PCA and cluster analysis methods, it is necessary to define and explain each variable used in statistical classification.

2.3.1 Variables

Six variables were retained for analysis in PCA and cluster analysis procedures. Area and thermal gradient are explained in greater detail in the following paragraph. The six variables are:

1. Lowest closed isobar in 1-hPa increments
2. Fastest 12-h intensification rate (hectopascals per hour) during storm's existence within the study region
3. Total area <1,004 hPa (square kilometers) at time of storm's maximum intensity
4. Sharpest thermal gradient (surface) 20°C to coldest isotherm (degrees Centigrade per 100 kilometers) at time of storm's maximum intensity
5. Formation region (numbered 1–5 from manual classification)
6. Hours within study region

Lowest closed pressure was chosen to be an indicator of absolute intensity as it is inversely proportional to wind

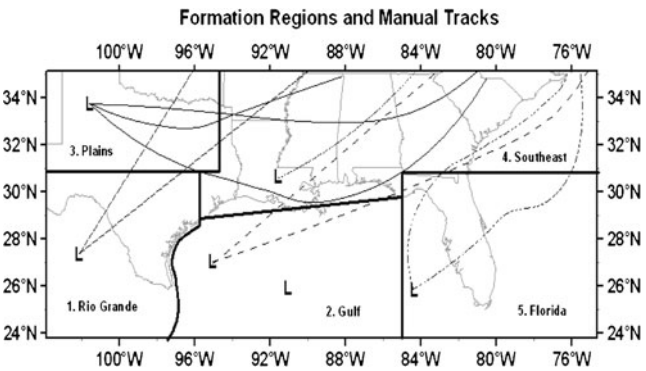

Fig. 2 Manual storm types and formation regions with common storm tracks

speed. Lowest closed pressure was obtained using 1-hPa contours and 6-h observations with NCEP reanalysis data. Area was selected as an important variable that is not often included in ETC climatologies. Storms occupying a larger area have the potential to impact a greater population. Calculating the area <1,004 hPa was more involved, requiring reanalysis data at 2.5°×2.5° to be extracted and clipped to the latitude and longitude coordinates defining the study region.

Using a GIS, the reanalysis values were spatially interpolated into a raster image at an interval of 4 hPa with inverse distance weighting (IDW) method using 50 nearest neighbors and a power of 2 (Daly et al. 2002). This spatial interpolation method produced surface isobar patterns almost identical to the online maps in the NCEP/NCAR Reanalysis website. Once imported and contoured, a blue/red color shading scheme was used to clearly define values <1,004 hPa. An area calculation tool was used segment by segment to measure the roughly circular perimeter of each storm on the 1,004 hPa contour line. The area <1,004 hPa was automatically calculated upon completing the roughly circular polygon. A value of 1,004 hPa was chosen in this step to differentiate between stronger ETCs and numerous ETCs with lowest pressures between 1,004 and 1,008 hPa. Furthermore, the concentric areas of many 1,008 hPa storms continued off the grid, making it more difficult to measure the areas of these marginal storms.

Thermal gradient was chosen because it has not been used in previous studies, and it ensures that all storms are extratropical. Thermal gradient was also assessed using a GIS. Reanalysis surface temperature data was extracted and contoured by 1-degree isotherms. Radii were measured from the storm center outward across the sharpest gradient of isotherms. To standardize the range of temperatures across different storms, the gradient was measured from the coldest isotherm, often 0°C, to the 20°C isotherm and recorded in °C/100 km. A 20°C isotherm was found in every storm. Although water temperatures at the southern margins of the grid occasionally approach the 19–22°C lower range for subtropical transition of an ETC (Roth 2002), all 84 storms were characterized by the presence of baroclinic zones on daily weather maps suggesting retention of ETC characteristics.

Total grid hours refers to the amount of time each storm existed within the boundaries of the study region. The first (last) recorded time from 6-h reanalysis intervals corresponded with the first (last) observation of a closed surface low <1,008 hPa with at least 75% of its circulation within the study region.

2.3.2 Principal components analysis

PCA was used to reduce the data to fewer transformed variables that capture the most significant component of variability in the observations. Using a single Varimax rotation, all components with eigenvalues over one were retained. The variables lowest closed pressure, intensification rate, and area loaded on component 1. Lowest closed pressure and intensification rate are strong predictors of intensity while larger storms trended towards higher intensity. Formation region and hours within study region were closely related and loaded on the second component. Thermal gradient loaded on both components, but favored component 2. These two components were then used in subsequent cluster analysis procedures.

2.3.3 Cluster analysis

Two types of cluster analysis were used to classify the transformed variables into storm types. Hierarchical cluster analysis was employed first, which is an agglomerative procedure preferred for smaller samples (Norusis 2010). We used the default settings in SPSS version 16.0 with between-groups linkage and squared Euclidean distance. The largest decrease in within-group variability was between six and seven clusters, suggesting that seven clusters should be retained. Hierarchical procedures are often used to determine structure and the number of clusters as an initial step prior to other types of cluster analysis (Norusis 2010). Furthermore, the effectiveness of non-hierarchical cluster procedures has proven to be superior in comparison (Gong and Richman 1995; Huth 1996; Huth et al. 2008). Here, we follow hierarchical clustering with k-means clustering, a non-hierarchical procedure. In k-means clustering, we predefined the number of groups at seven, as determined by hierarchical clustering. Our statistical classification uses the results of k-means clustering with seven groups.

2.4 GIS precipitation analysis

Cumulative precipitation totals for each storm were obtained from NOAA/National Climatic Data Center's (NCDC's) station locator webpage (http://lwf.ncdc.noaa.gov/oa/climate/stationlocator.html) for a set of 13 selected cities with approximate equidistant spacing within the study region. Since there were several different storm types moving across 30° of longitude, the starting and ending time of precipitation varied at each location for each storm. For lack of a better method, each of the cumulative storm precipitation totals for all 84 storms were evaluated separately at each of the 13 locations, producing 1,092 cases. Precipitation was recorded in traditional 24-h days from the NOAA/NCDC station locator website, and totals were summed for each storm by synchronizing the 24-h totals with the position of the low using the previously mentioned NCEP/NCAR Reanalysis dataset in 6-h increments and also NOAA daily weather maps. This procedure of comparing

precipitation totals with the position of the ETC using NCEP/NCAR Reanalysis and NOAA daily weather maps ensured that storm precipitation was attributed to the impacts of each storm and not other synoptic scale influences.

Median precipitation values were then calculated for each storm type at each location and mapped using a GIS. Median values were chosen instead of mean values for several reasons: (1) unequal group membership among storm types, (2) very small sample sizes for certain storm types, and (3) potential outlier values possibly attributed to mesoscale processes. The median precipitation values were spatially interpolated into a raster image with IDW method using 50 nearest neighbors and a power of 6. A power of 6 was chosen to place more emphasis on nearby points and increase resolution for precipitation interpolation (Gemmer et al. 2004).

3 Results and discussion

3.1 Manual classification

Manual classification was performed due to its simplicity and its spatial representation of genesis regions. There are some interesting relationships between the five manual regions, decadal frequency, and ENSO phase. Of the five regions, the Gulf region is the most common with 24 storms followed by Plains and Rio Grande (Table 1). Storm formation is more common on the western side of the study region with only 25% of storms originating in regions 4 and 5 (see Fig. 2). Decadal frequency shifts among formation regions and is also associated with ENSO events. Eight out of ten Florida storms were observed in the 1970s and 1980s, while the 1970s was the most common decade for southeastern storms (Fig. 3). Only six Southeastern and Florida storms combined have formed since 1990. One hypothesis for the lack of Southeastern and Florida storms since 1990 is suppressed cyclogenesis related to variability in the North Atlantic High. The 1970s was the most active decade with 26 storms. While Southeast, Florida, and Plains storms were more frequent in the 1970s, Rio Grande storms have been more numerous in recent years. Relationships with ENSO are discussed in a later section. Future research will analyze possible explanations for shifts in formation regions over decadal time periods.

3.2 Statistical classification

PCA followed by k-means cluster analysis with seven groups effectively classified southern ETCs into one of seven types. The seven types contained combinations of varying properties. Some groups appeared to have common geographical characteristics. Others were classified primarily by intensity, duration, or size. While the clustering procedure was objective, interpreting and naming the seven groups into storm types is a subjective process at the authors' discretion. In order to maintain consistency, we adopted a naming convention similar to the Köeppen system where a capital letter is used followed by one to two lower-case letters. The capital letters in our naming method denote the dominant geographic location, or unique storm characteristics. The capital letters are sometimes followed by lower-case letters referring to size, intensity, or both. A brief explanation of each type is presented below with a visual representation of a notable storm from each group at its maximum intensity (Fig. 4). Table 2 summarizes the mean and median characteristics for each variable for each storm type. The seven storm types are:

1. Wli (Western large intense, 5 total)—These storms are the largest and most intense type of southern ETC. The rate of intensification is the second fastest among all seven types, and the duration is also second longest. Wli are possibly the most influential type of southern ETC due to the long duration and large size. The strongest member of the group is 03/17/83, a Gulf storm, which is also by far the largest of all 84 storms, and the second most intense.
2. Es (Eastern small, 18 total)—These are small storms that do not intensify rapidly and are also typified by

Table 1 Cross-tabulation of manual and statistical storm types

Storm type	Formation region					Total
	Rio Grande	Gulf	Plains	Southeast	Florida	
Wli	1	3	1	0	0	5
Es	1	1	4	8	4	18
SM	1	4	2	0	0	7
Ws	8	7	7	1	1	24
RI	0	0	0	2	4	6
SS	0	1	0	0	0	1
Wm	6	8	8	0	1	23
Total	17	24	22	11	10	84

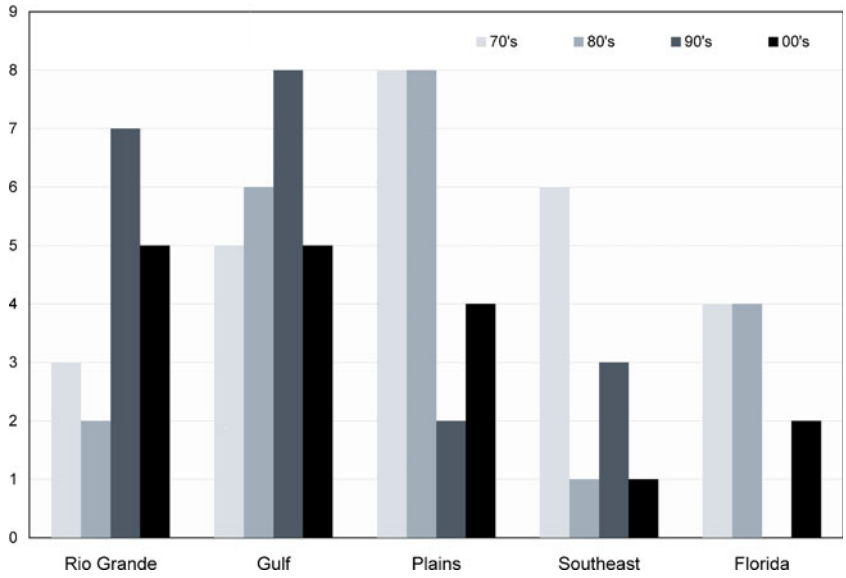

Fig. 3 Count of manual storm types per decade

shorter durations. This type commonly forms in the Southeast region (8/18), or in the Florida region (4/18). This type may also form in the Plains and track eastward into the Southeast. The strongest and largest member of the group is 02/09/78, a Southeastern storm.

3. SM (Slow-mover, 7 total)—These storms are generally of moderate intensity and size, but exhibit the longest durations of any group. The most intense, largest, and longest-lived member of this group is 02/06/92, a Gulf storm.
4. Ws (Western small, 24 total)—Similar to Es in almost every characteristic, Ws are generally slightly smaller than Es but of longer duration due to a more westward formation location. The strongest member of this group is 01/01/03.
5. RI (Rapid-intensification, 6 total)—These types of storms are moderate in size and intensity. RI storms are short-lived with most forming on the extreme eastern side of the study region in coastal waters near Florida or over the Southeast. Central pressures decrease rapidly as RI's track up the east coast or into the Atlantic. The strongest member of this group is 01/22/87.

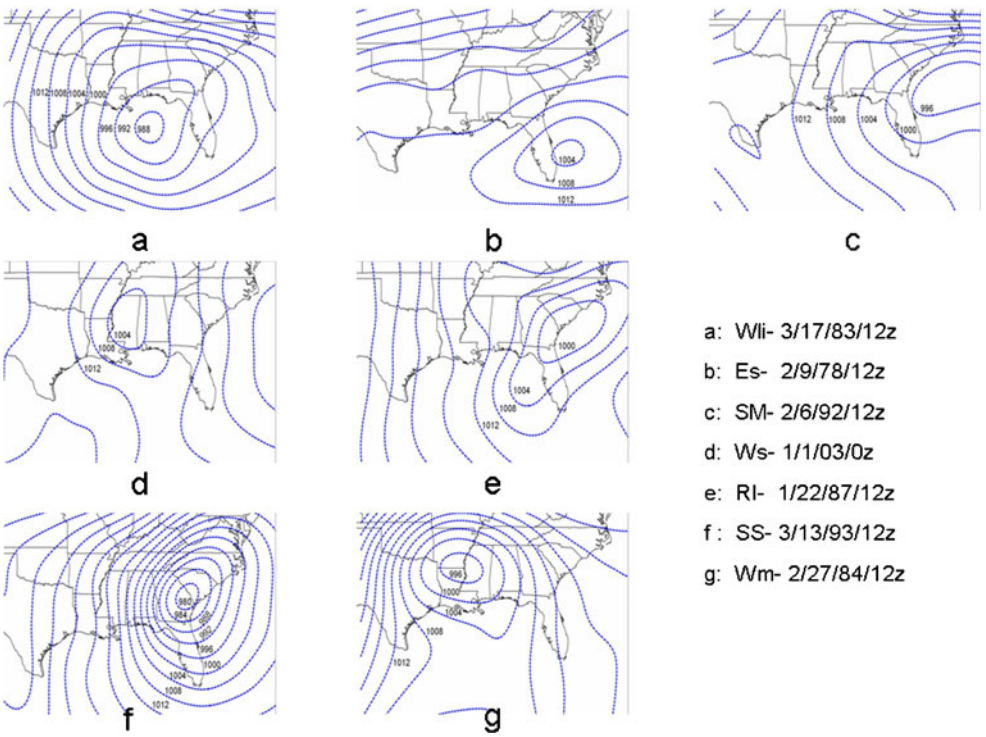

Fig. 4 Example of the most intense statistical storm type in each group. Each storm was captured at maximum intensity. Thus, a western storm may not have achieved maximum intensity until it was on the eastern edge of the study region

Table 2 Mean and median characteristics for each statistical storm type

Variable	Wli (5)		Es (18)		SM (7)	
	Mean	Median	Mean	Median	Mean	Median
Lowest closed hPa	990	991	1,003	1,003	1,000	1,000
Intensification rate (hPa/h)	0.58	0.50	0.16	0.17	0.25	0.17
Area (km^2) <1,004 hPa	2.47×10^6	2.28×10^6	2.5×10^5	1.61×10^5	7.43×10^5	6.99×10^5
Thermal gradient (°C/100 km)	1.6	1.6	2.7	2	1.1	1
Hours within study region	34	30	17	15	53	54
Formation region	2	2	3.7	4	2.1	2
	Ws (24)		RI (6)		Wm (23)	
Lowest closed hPa	1,003	1,003	999	999	998	998
Intensification rate (hPa/h)	0.16	0.17	0.61	0.63	0.38	0.42
Area (km^2) <1,004 hPa	2.1×10^5	2.1×10^5	8.3×10^5	7.5×10^5	9.9×10^5	8.9×10^5
Thermal gradient (°C/100 km)	2.1	2.1	2.5	2.5	1.8	1.8
Hours within study region	25	24	12	12	24	24
Formation region	2.2	2	4.7	5	2.2	2
Lowest closed hPa	SS(1) 979					
Intensification rate (hPa/h)	1.5					
Area (km^2) <1,004 hPa	2.1×10^6					
Thermal gradient (°C/100 km)	3					
Hours within study region	18					
Formation region	2					

6. SS (Superstorm, 1 total)—This group is represented by only one storm 03/13/93. Using hierarchical cluster analysis and a range of solutions, the March 1993 superstorm is so unique that it was not merged with another cluster until forcing a two-group solution. It is frequently referred to as the storm of the century in the United States, and its monumental characteristics are best summarized in Kocin et al. (1995). The March superstorm is the only storm with a pressure <980 hPa, the only storm to intensify at a rate >1 hPa/h, and also one of the five largest storms in the study.
7. Wm (Western moderate, 23 total)—This group is aptly named for its moderate characteristics in every category. These storms are more intense than every type except for SS and Wli. The intensification rate for Wm trails Mss, RI, and Wli while the size is also third. The distribution is split almost equally between Rio Grande, Gulf, and Plains storms. The strongest member of the group is 2/27/84.

3.3 Relationships with ENSO

Southern ETCs are more frequent during El Niño episodes (Schubert et al. 2008). Using the Oceanic Niño Index (ONI), a running mean of the Niño 3.4 region, seasonal frequency was evaluated for both statistical and manual storm types (Figs. 5 and 6). The ONI defines a strong El Niño episode as at least three consecutive months ≥1.5°C+SST anomaly. The most active southern ETC seasons were associated with strong El Niño in 1982–1983 (seven storms) and 1997–1998 (six storms). A moderate El Niño in 1986–1987 also produced seven storms. Moderate and strong El Niño episodes occur in conjunction with 32/84 storms which suggests a positive relationship with strong ETCs in the southern United States. This is especially true for Gulf storms and Wli, Wm, and SM storms (Figs. 5 and 6). During strong to moderate El Niño, there were 13/24 Gulf storms, 3/5 Wli, 11/23 Wm, 3/7 SM, and 8/24 Ws. Since the percentages are higher for the stronger Wli, Wm, and SM, it appears that stronger El Niño tends to show a positive relationship with more intense southern ETCs. However, it should be noted that a moderate El Niño in 1994–1995 occurred with no storms, and a strong El Niño occurred in 1991–1992 with only two storms.

Conversely, strong La Niña episodes are associated with fewer storms (Figs. 5 and 6), but, with only three events, this is inconclusive. There have been seven strong and moderate La Niña episodes combined, and these seasons are associated with only 12 storms. Curiously, Es is a storm type that appears to slightly favor La Niña for development (Fig. 6), and this could indicate a localized area of cyclogenesis near coastal South Carolina and Georgia (Curtis 2006). Strong ENSO phases influence the probability of increased or decreased southern ETC occurrence, although it should be noted that the small sample size of strong ENSO phases decreases the legitimacy of these conclusions.

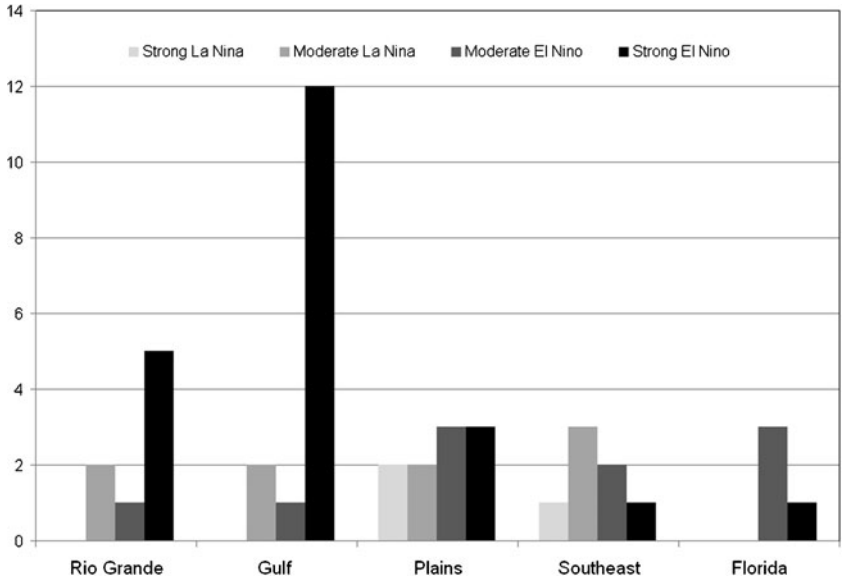

Fig. 5 Count of manual storm types by ENSO phase

3.4 Hydrometeorological analysis

While the majority of this article is devoted to the ETC classification scheme, the most important results are possibly mapping median precipitation for each storm type. Forecasters may be able to refer to this research and to individual analog storms in order to more accurately estimate expected precipitation for future ETCs.

Median precipitation was calculated at each location for each storm type. Both statistical and manual types of storms show distinct spatial precipitation swaths. For the manual storms, the precipitation swath serves as a proxy for mean storm track and position of the low center. Tracks vary considerably for the statistical storms; however, median precipitation swaths indicate unique precipitation signatures. Generally, precipitation is lighter on the western side of the grid closer to the formation region for all storms. Precipitation totals increase as storms progress east or northeast and advect Gulf of Mexico moisture into the southeast.

3.4.1 Manual storm type precipitation

The discussion of manual precipitation results begins on the western side of the grid with Plains Lows. Plains Lows generally track west to east and then display a northeastward curvature in the vicinity of 89 or 88°W longitude (see Fig. 2). A median maxima occurs in the Florida Panhandle with 38 mm in Tallahassee, FL, and 36 mm in Mobile, Al (Fig. 7). Southern Texas rarely receives measurable precipitation from Plains Lows. The Florida peninsula is commonly

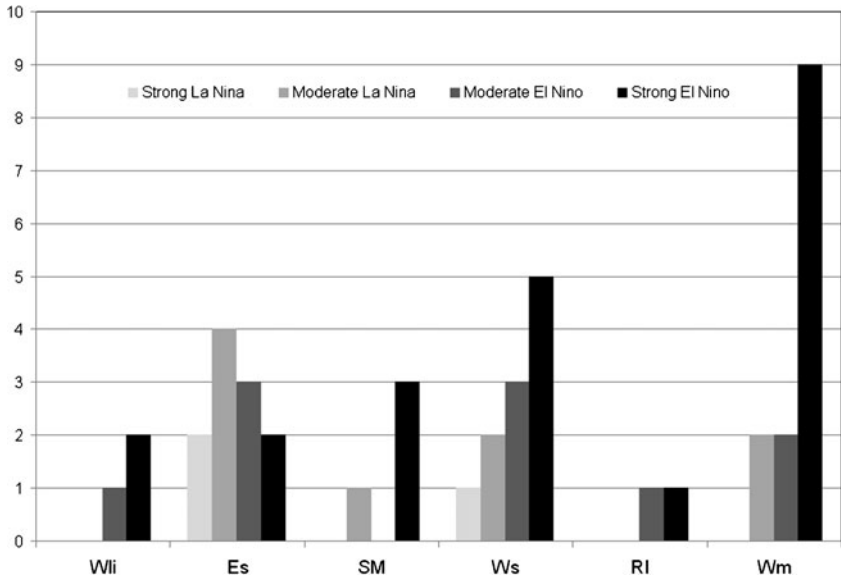

Fig. 6 Count of statistical storm types by ENSO phase

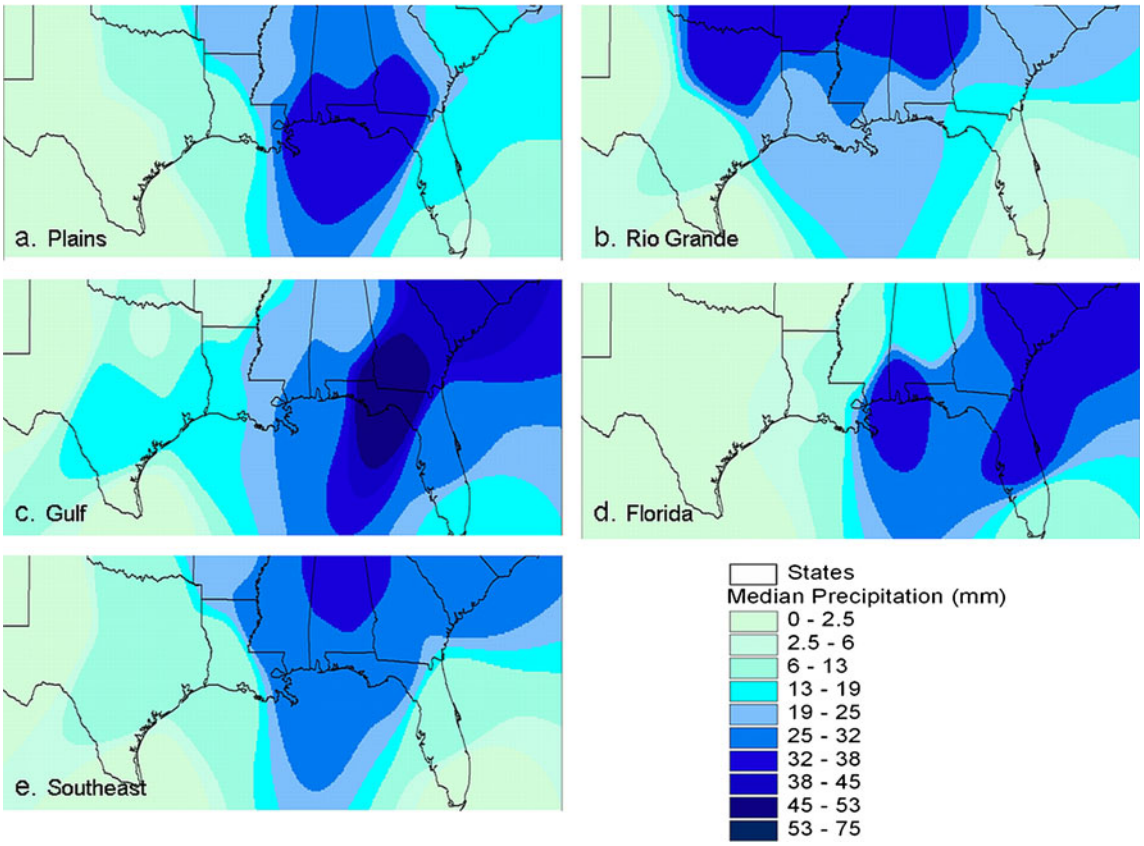

Fig. 7 Median precipitation for manual storm types: (**a**) Plains, (**b**) Rio Grande, (**c**) Gulf, (**d**) Florida, (**e**) Southeast

transited by a trailing cold front when a Plains Low travels towards New England. A trailing cold front may occasionally produce heavy precipitation in Orlando but often does not have enough momentum to impact Miami.

Rio Grande lows form in the Rio Grande Valley region and track NNE toward the Great Lakes or NE towards New England. Not surprisingly, these storms inundate locations on the northern edge of the study region as they begin to intensify. A dual median maxima of 36 mm occurs at Dallas, TX, and Birmingham, AL. Rio Grande Lows produce the second most precipitation per location of the five manual types. Although originating near Brownsville, TX, very little precipitation falls in South Texas from Rio Grande Lows.

Gulf lows produce the most total precipitation and also the highest median precipitation per location. Gulf lows have a very distinct precipitation swath that is closely aligned with the tracks of these systems. A median maxima of 51 mm occurs at Tallahassee, FL, with a continuation of higher values through Georgia, South Carolina, and the eastern coast of the United States.

Florida lows display a similar pattern to Gulf lows, albeit, the swath is farther east with a maxima of 38 mm in Columbia, SC. Florida lows are too far east to produce heavy precipitation over Texas, although some Florida lows develop off the coast of the Florida Panhandle and create extensive wraparound precipitation on the Gulf coast. Southeastern lows form and then quickly move out of the grid. A maxima of 34 mm occurs near Birmingham, AL.

3.4.2 Statistical storm type precipitation

Unlike the manual storms, statistical storms do not have precipitation swaths that serve as proxies for track position. Statistical storms are classified by their general formation location and characteristics; nevertheless, median precipitation totals for the statistical storms also display swaths of precipitation with subtle spatial differences and distinct intensity gradients (Fig. 8). Most statistical storm types produce slightly less precipitation per location when compared with the manual types. Notable exceptions are Wli and Wm, which generated the highest per location yields of any storm types.

There were only five Wli storms in the dataset, and these large storms occupy much of the study region with median central pressures of 990 hPa. Three of the five Wli storms are Gulf storms, which partially explains why Columbia, SC, and Tallahassee, FL, receive median values of 72 and 65 mm. Unlike storms of weaker intensities, Wli storms are strong enough to pull a trailing cold front into southern

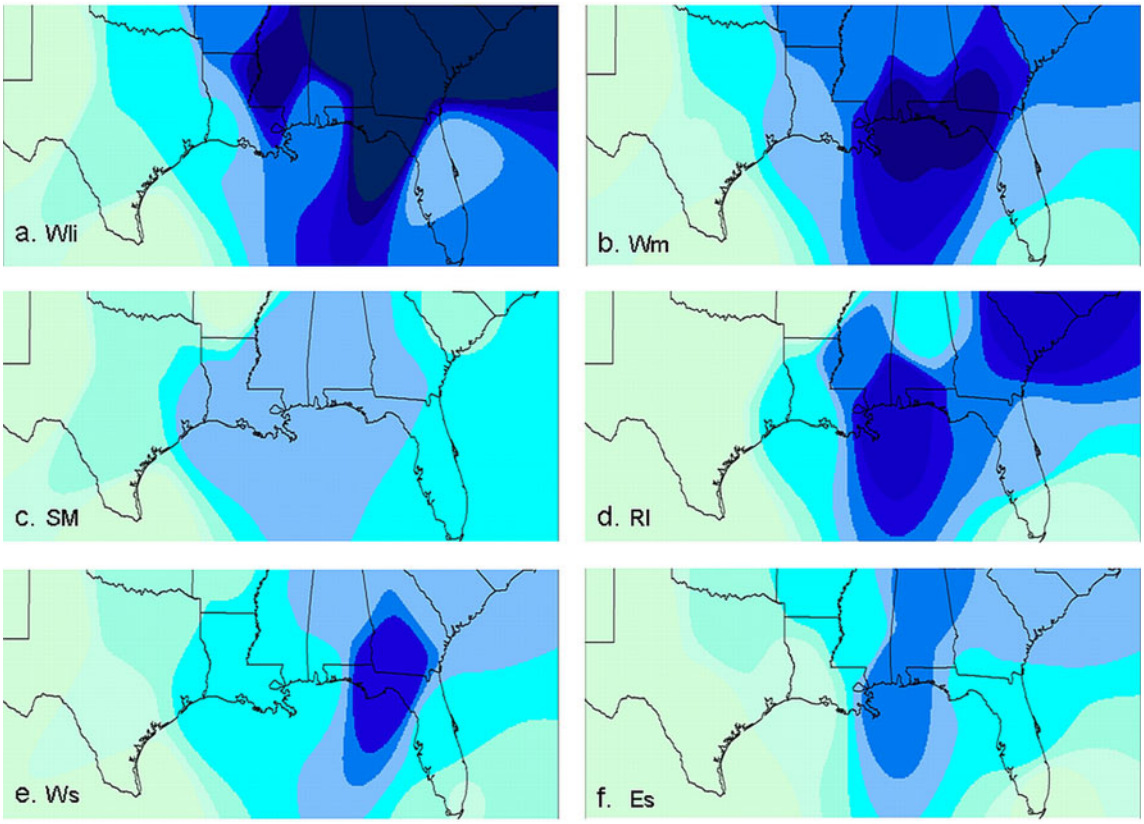

Fig. 8 Median precipitation for statistical storm types: (**a**) Wli, (**b**) Wm, (**c**) SM, (**d**) RI, (**e**) Ws, (**f**) Es. Refer to Fig. 7 for the legend

Florida. Wm storms supplied the Gulf Coast with more precipitation while also concentrating on inland locations. Tallahassee, FL, and Mobile, AL, were most impacted with 47 mm of precipitation from Wm storms.

Ws and SM storms yield similar spatial swaths of precipitation. Curiously, the SM storms have lower precipitation totals than many other types, despite their longer residence time in the study region. Although Ws storms do not contain much precipitation, these types of storms delivered precipitation to all cities within the study region.

RI storms have two primary formation locations followed by rapid intensification. The first location is in the northern Gulf off the coast of the Florida panhandle. This possibly explains why Mobile, AL, has a maxima of 44 mm. The second location is near the Gulf or Atlantic coast of the Florida peninsula. Most Es storms are also southeastern storms, and the resulting precipitation distribution has many shared characteristics between the two storm types.

4 Conclusions

Southern ETCs are often overlooked when compared with tropical cyclones in the region and ETCs in the northern United States. It is important to have an operational scheme in place for identifying, analyzing, and discussing these nameless storms. Furthermore, southern ETCs make an important contribution to the water budget of the region by providing valuable precipitation during the cool season recharge months. It is therefore important for weather and hydrologic forecasters to develop an understanding of the amounts of precipitation that can be attributed to types of ETCs in the region.

In this research, we classified southern ETCs using both manual and statistical techniques. By analyzing 40 years of daily weather maps, we identified five distinct manual formation regions for ETCs that produce unique tracks either eastward or northeastward. These manual regions are: (1) Rio Grande, (2) Gulf, (3) Plains, (4) Southeast, and (5) Florida. A statistical classification was also performed using PCA with six variables and 84 storms. This was followed by hierarchical and then k-means cluster analysis. The final results of k-means cluster analysis produced seven distinct storm types. We adopted a naming scheme similar to climatic classification where an upper-case letter denotes geographic location or unique characteristics, and lower-case letters refer to size and intensity. The seven automated storm types are: (1) (Wli) Western large intense, (2) (Es) Eastern small, (3) (SM) Slow-mover, (4) (Ws) Western small, (5) (RI) Rapid-intensification, (6) (SS) Superstorm, and (7) (Wm) Western moderate.

Both manual and statistical storm types generally displayed positive (negative) associations with El Niño (La Niña). The most active ETC seasons in the southeastern United States were associated with strong El Niño episodes in 1982–1983, 1997–1988, and with a moderate El Niño in 1986–1987. Furthermore, strong El Niño episodes tend to produce a higher frequency of intense southern ETCs. Cumulatively, only 12 storms formed in the seven episodes of at least moderate La Niña conditions.

After classifying storms both manually and statistically, we analyzed the median precipitation that each storm type produced at 13 evenly spaced cities within the study region. Median precipitation was chosen because of unequal group membership among storm types and small sample sizes. A GIS was then used to interpolate precipitation values to map areas of precipitation for each storm type.

The manual storm types were characterized by unique swaths of spatial precipitation that further substantiate the exclusivity of the five manual tracks. Of these types of storms, Gulf ETCs supply the most precipitation per location. The statistical storm types were distinguished less by track and more by precipitation intensity. Of these types of storms, the Western large intense ETCs supplied the most precipitation per location.

It is hoped that the results of this research will assist hydrologists and weather forecasters by providing an analog of case studies to better estimate precipitation amounts for future southeastern ETCs. It is also hoped that the classification schemes presented here will offer broadcast meteorologists a mechanism to refer to ETCs so that they may better communicate with their viewers and listeners. Future research will focus on weather hazards created by types of southern ETCs and also on cyclogenesis processes for each storm type.

Since two classification methods are presented, it is suggested that both methods should be used in conjunction for operational purposes. Manual storm types are more valuable for prediction in real and near time while statistical storm typing is more beneficial in post event analysis. Nevertheless, statistical storm classification can be estimated in real and near time to supplement predictions of precipitation amounts using manual storm typing.

Acknowledgment The authors would like to thank anonymous reviewers for their helpful criticism and insight in improving this manuscript.

References

Bartholy J et al (2006) European cyclone track analysis based on ECMWF ERA-40 data sets. Int J Climatol 26:1517–1527

Bernardes Pezza A, Ambrizzi T (2005) Dynamical conditions and synoptic tracks associated with different types of cold surge over tropical South America. Int J Climatol 25:215–241

Bierly GD, Winkler JA (2001) A composite analysis of airstreams within cold-season Colorado cyclones. Weather Forecast 16:57–80

Bowie EH, Weightman RH (1914) Types of storms of the United States and their average movement. Mon Weather Rev 42:3–37

Buckley BW, Leslie LM (2004) Preliminary climatology and improved modelling of south Indian Ocean and Southern Ocean mid-latitude cyclones. Int J Climatol 24:1211–1230

Businger S et al (1990) Storm following climatology of precipitation associated with winter cyclones originating over the Gulf-of-Mexico. Weather Forecast 5:378–403

Campins J et al (2000) A catalogue and a classification of surface cyclones for the Western Mediterranean. Int J Climatol 20:969–984

Campins J et al (2010) Climatology of Mediterranean cyclones using the ERA-40 dataset. Int J Climatol. doi:10.1002/joc.2183

Changnon SA (2007) Catastrophic winter storms: an escalating problem. Clim Chang 84:131–139

Colucci SJ (1976) Winter cyclone frequencies over the Eastern United States and adjacent Western Atlantic. Bull Am Meteorol Soc 57:548–553

Curtis S (2006) Developing a climatology of the South's 'other' storm season: ENSO impacts on winter extratropical cyclongenesis. Southeast Geogr 46:231–244

Daly C, Gibson WP, Taylor GH, Johnson GL, Pasteris P (2002) A knowledge-based approach to the statistical mapping of climate. Clim Res 22:99–113

Davis RE et al (1993) Synoptic climatology of Atlantic coast Northeasters. Int J Climatol 13:171–189

Eichler T, Higgins W (2006) Climatology and ENSO-related variability of North American extratropical cyclone activity. J Climate 19:2076–2093

Esteban P et al (2006) Daily atmospheric circulation catalogue for Western Europe using multivariate techniques. Int J Climatol 26:1501–1515

Fragoso M, Gomes PT (2008) Classification of daily abundant rainfall patterns and associated large-scale atmospheric circulation types in Southern Portugal. Int J Climatol 28:537–544

Frankoski NJ, DeGaetano AT (2011) An East Coast winter storm precipitation climatology. Int J Climatol 31:802–814

Froude LSR et al (2007) The predictability of extratropical storm tracks and the sensitivity of their prediction to the observing system. Mon Weather Rev 135:315–333

Gamble DW (1997) The relationship between drainage basin area and annual peak flood seasonality in the Southeastern United States. Southeast Geogr 37:61–75

Gemmer MS, Becker S, Jiang T (2004) Observed monthly precipitation trends in China 1951–2002. Theor Appl Climatol 77:39–45

Gong XF, Richman MB (1995) On the application of cluster analysis to growing season precipitation data in North American east of the Rockies. J Climate 8:897–931

Hart M et al (2006) A synoptic climatology of tropospheric ozone episodes in Sydney, Australia. Int J Climatol 26:1635–1649

Hayden, BP (1988) Flood climates. In: VR Baker, RC Kochel, and PC Patton (eds), Flood geomorphology (New York, NY: John Wiley and Sons)

Hirsch ME, DeGaetano AT, Colucci SJ (2001) An East Coast winter storm climatology. J Climate 14:882–899

Hirschboeck, KK (1991) The role of climate in the generation of floods. In: RW Paulson, EB Chase, RS Roberts, and DW Moody (eds.) National water summary 1988–1989 USGS Water Supply Paper 2375. Denver, CO: USGS

Huth R (1996) An intercomparison of computer-assisted circulation classification methods. Int J Climatol 16:893–922

Huth R et al (2008) Classification of atmospheric circulation patterns—recent advances and applications. Ann N Y Acad Sci 1146:105–152

Kalnay E et al (1996) The NCEP/NCAR 40-year reanalysis project. Bull Am Meteorol Soc 77:437–471

Klein WH (1957) Principal tracks and mean frequencies of cyclones and anticyclones in the northern hemisphere. Research Paper 40, U.S. Weather Bureau: 60 pp

Kocin PJ, Uccellini LW (2004) A snowfall impact scale derived from Northeast storm snowfall distributions. Bull Am Meteorol Soc 85:177–194

Kocin PJ et al (1995) Overview of the 12–14 March 1993 Superstorm. Bull Am Meteorol Soc 76:165–182

Kouroutzoglou J et al (2010) Climatological aspects of explosive cyclones in the Mediterranean. Int J Climatol. doi:10.1002/joc.2203

Kunkel KE et al (1999) Temporal fluctuations in weather and climate extremes that cause economic and human health impacts: a review. Bull Am Meteorol Soc 80:1077–1098

Lewis JK, Hsu SA (1992) Mesoscale air-sea interactions related to tropical and extratropical storms in the Gulf of Mexico. J Geophys Res 97:2215–2228

Maheras P et al (2001) A 40 year objective climatology of surface cyclones in the Mediterranean region: spatial and temporal distribution. Int J Climatol 21:109–130

Mennis J (2001) Exploring relationships between ENSO and vegetation vigour in the south-east USA using AVHRR data. Int J Remote Sens 22:294–311

Mesquita MS et al (2010) Characteristics and variability of storm tracks in the North Pacific, Bering Sea, and Alaska. J Climate 23:294–311

Neal RA, Phillips ID (2009) Summer daily precipitation variability over the East Anglian region of Great Britain. Int J Climatol 29:1661–1679

Norusis MJ (2010) PASW statistics 18 statistical procedures companion. 656 pp

Peters AJ, Ji L, Walter-Shea E (2003) Southeastern U.S. vegetation response to ENSO events (1989–1999). Clim Chang 60:175–188

Pettersen S (1956) Weather analysis and forecasting. McGraw-Hill, New York, NY. 422 pp

Raible CC et al (2008) Northern hemisphere extratropical cyclones: a comparison of detection and tracking methods and different reanalyses. Mon Weather Rev 136:880–897

Reitan CH (1974) Frequencies of cyclones and cyclogenesis for North America, 1951–1970. Mon Weather Rev 102:861–868

Roth DM (2002) A fifty year history of subtropical cyclones. 25th Conference on Hurricanes and Tropical Meteorology, P1.43

Schubert SD et al (2008) ENSO and wintertime extreme precipitation events over the contiguous United States. J Climate 21:22–39

Sheridan SC et al (2008) A further analysis of the spatio-temporal variability in aerosols across North America: incorporation of lower tropospheric (850-hPa) flow. Int J Climatol 28:1189–1199

Simmonds I, Keay K (2000) Mean southern hemisphere extratropical cyclone behavior in the 40-year NCEP-NCAR reanalysis. J Climate 13:873–885

Thomas BC, Martin JE (2010) A synoptic climatology and composite analysis of the Alberta Clipper. Weather Forecast 22:315–333

Wernli H, Schwierz C (2006) Surface cyclones in the ERA-40 dataset (1958–2001). Part I: novel identification method and global climatology. J Atmos Sci 63:2486–2507

Whittaker LM, Horn LH (1981) Geographical and seasonal distribution of North American cyclogenesis, 1958–1977. Mon Weather Rev 109:2312–2322

Whittaker LM, Horn LH (1984) Northern hemisphere extratropical cyclone activity for four mid-season months. Int J Climatol 4:297–310

Zielinski GA (2002) A classification scheme for winter storms in the Eastern and Central United States with an emphasis on Nor'easters. Bull Am Meteorol Soc 83:37–51

Zishka KM, Smith PJ (1980) The climatology of cyclones and anticyclones over North America and surrounding ocean environs for January and July, 1950–77. Mon Weather Rev 108:387–401